ROYAL SOCIETY OF CHEMISTRY

PAPER

Check for updates

A "turn-on" chemodosimeter for detection of Cu²⁺ in living cells

Marlies Körber,* Dina Attia, Elisabeth Kohlbauer-Masson [ID] and Andriy Mokhir [ID] *

We synthesized an analogue of rhodamine B hydrazide *via* alkylation with butyl bromide. The resulting reagent, BuCh, exhibits optimal lipophilicity, maintaining both aqueous solubility and efficient cell membrane permeability. BuCh itself is weakly fluorescent, but in the presence of Cu²⁺ it undergoes hydrolysis to release strongly fluorescent rhodamine B. We demonstrated that BuCh is well suited for monitoring chelatable intracellular Cu²⁺ ions in mammalian cells.

Introduction

Copper is an essential trace element in the human body and, after iron and zinc, one of the most abundant transition metals. Copper ions (Cu⁺ and Cu²⁺) function as crucial catalytic cofactors in a range of redox-active enzymes, including superoxide dismutase (SOD), ferroxidase, and tyrosinase, and are thus integral to various enzymatic processes and electron transport pathways.[1–3] Dysregulation of copper homeostasis can lead to oxidative stress and associated cytotoxic effects in the event of copper overload and, in the event of copper deficiency, can cause critical disruptions to many biological processes.[4–6] Such imbalances have been implicated in the pathogenesis of several neurodegenerative disorders, including Menkes syndrome, Wilson's disease, and Alzheimer's disease.[7–10] An alteration in copper level was also found in the blood and serum of patients with various types of cancer, such as colorectal, thyroid, gallbladder, and breast cancer.[11–14] Therefore, there is a great need for a detection of Cu ions in a non-invasive way directly in living cells, *e.g.* by monitoring fluorescence. Excellent fluorogenic probes and chemodosimeters for detection of Cu⁺ in living cells are already known.[15–18] Some of them are even commercially available: Coppersensor 1 (CS1, MedChemExpress) and CooperGREEN™ (GORYOChemical). In contrast, Cu²⁺ monitoring is less well established. Since Cu²⁺ is a strong quencher of fluorescence of organic dyes, most known Cu²⁺ probes are "turn-off" systems.[19–22] Due to the high background fluorescence of these probes, their use is prone to false positives and low to moderate sensitivity towards Cu²⁺. In recent years, considerable progress has been made in the development of so-called "turn-on" fluorescent probes with high selectivity and sensi-

tivity for Cu²⁺.[23–26] Common examples include probes based on coumarin, fluorescein, boron dipyrromethene (BODIPY), naphthalimide and rhodamine derivatives.[23] Cu²⁺ can be also detected by using activity based sensing probes developed by Chang and colleagues in combination with fluorescence microscopy.[27] However, the known Cu²⁺ probes are often complex molecules, which are not broadly accessible.[18,28–34] Correspondingly, no reliable fluorogenic probes for detection of Cu²⁺ in living cells are commercially available yet.

In 1997, Czarnik *et al.* introduced rhodamine B hydrazide (HCh) as a very simple Cu²⁺ chemodosimeter in aqueous, cell-free systems. Its function relies on the fact that Cu²⁺ catalyzes the conversion of HCh to fluorescent rhodamine B at rates far exceeding those induced by other metal ions (Scheme 1A).[35]
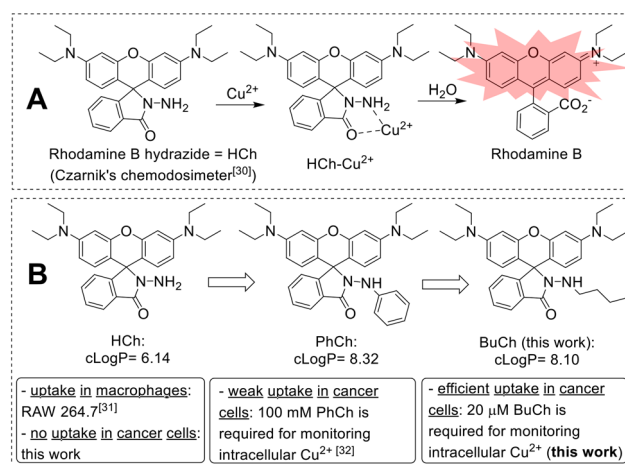
Scheme 1 (A) Mechanism of Cu²⁺-mediated hydrolysis of non-fluorescent Czarnik's chemodosimeter (HCh) with formation of fluorescent rhodamine B. (B) Structures and calculated logarithms of *n*-octane/water partition coefficients (clog*P*) of HCh and its analogues PhCh[32] and BuCh (this work).

Friedrich-Alexander-University of Erlangen-Nürnberg (FAU), Department of Chemistry and Pharmacy, Organic Chemistry II, 91058 Erlangen, Germany. E-mail: andriy.mokhir@fau.de, ripplmarlies@gmail.com

However, despite its relatively high lipophilicity (clog P = 6.14), HCh is not cell membrane permeable with few exceptions. In particular, it has been reported that HCh can be applied for monitoring nitrogen oxide in murine RAW 264.7 macrophages.[36] The uptake improvement could be achieved by introduction of an N-phenyl residue to HCh to obtain reagent PhCh (clog P = 8.32, Scheme 1B).[37] PhCh was found to be suitable for monitoring intracellular Cu^{2+} in breast cancer MCF-7 cells by using fluorescence microscopy. However, a very high concentration of the reagent PhCh (0.1 M) is necessary to obtain the reliable signal to noise ratio indicating that the cellular uptake of PhCh is still not efficient.

In this work, we improved properties of Cu^{2+} chemodosimeters based on rhodamine B hydrazide by replacing the phenyl moiety with a butyl moiety. The resulting reagent BuCh is soluble in aqueous solutions and does not aggregate up to the concentration of 20 μM. It has optimal lipophilicity that enables its efficient cell membrane permeability and, therefore, allows reliable monitoring of chelatable Cu^{2+} pool in mammalian cell lines.

Results and discussion

Synthesis

BuCh was synthesized in two steps (Scheme 2). First, rhodamine B was reacted with hydrazine hydrate in ethanol to yield rhodamine B hydrazide. This intermediate was subsequently alkylated with 1-bromobutane in the presence of Cs_2CO_3 and CsI in N,N-dimethylformamide (DMF). After purification by column chromatography on aluminum oxide, BuCh was isolated as a dihydrate in 50% yield (Scheme 2). Identity of the product was confirmed by ^1H and ^{13}C NMR spectroscopy as well as high-resolution atmospheric pressure photoionization mass spectrometry (HR-APPI MS). Elemental analysis (C, H, N) verified a purity exceeding 95% (Fig. S1–4).

Lipophilicity of BuCh, its solubility and aggregation behaviour in aqueous solutions

We hypothesized that the excessive lipophilicity of PhCh promotes aggregation in aqueous solution, thereby impairing its cell membrane permeability. To address this limitation, we introduced a butyl substituent to obtain BuCh, whose lipophilicity falls between that of HCh and PhCh according to calculated clog P values (Scheme 1B). The experimentally determined log P of BuCh was 6.24 ± 0.06 (Fig. S8 and S9), which is
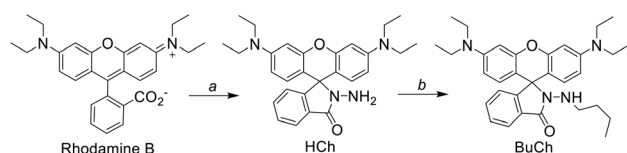
lower than the calculated value. This discrepancy likely reflects partial protonation of BuCh in aqueous solution, giving rise to less lipophilic species. Consistent with this interpretation, BuCh displayed good solubility in aqueous media, including phosphate-buffered saline (PBS, 10 mM, pH 7.4) up to 20 μM (Fig. S5–S7).

Using dynamic light scattering (DLS), we observed that the PBS medium routinely used in our laboratory contains particulates with broadly distributed sizes ranging from 32 to 186 nm, likely corresponding to airborne dust contamination. Particulates of similar sizes (131–199 nm) were also detected in PBS solutions containing BuCh at concentrations of 0–20 μM, with no statistically significant difference compared to PBS alone (Student's t-test, p > 0.05). In contrast, at 25 μM BuCh, larger particulates (620–1240 nm) were detected; however, this difference relative to PBS was not statistically significant (p = 0.09) (Fig. 1). These findings indicate that BuCh remains predominantly in its monomeric form in aqueous solution at concentrations up to 20 μM, consistent with solubility measurements.

Reaction of BuCh with Cu^{2+} in cell free settings
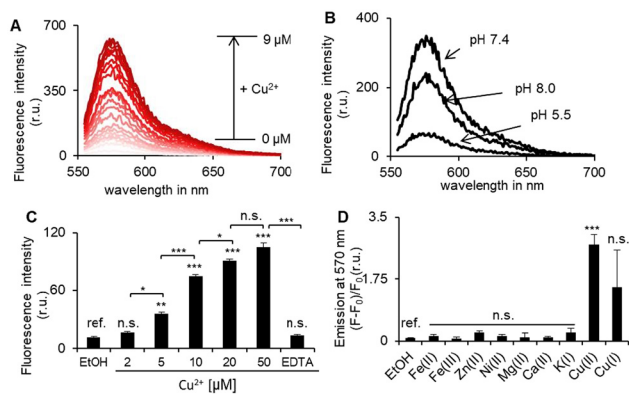
BuCh (20 μM) is weakly fluorescent when dissolved in PBS (10 mM, pH 7.4) similarly to its known analogues HCh and PhCh: F_0 = 27 relative units (r.u.), excitation wavelength λ_{ex} = 540 nm, emission wavelngth λ_{em} = 570 nm (Fig. 2). A dose dependent fluorescence increase is observed after addition of copper(II) acetate ($Cu(OAc)_2$: 0–9 μM) to BuCh and short incubation of 10 min. In particular, after addition of $Cu(OAc)_2$ (0.5, 5 or 9 μM) to BuCh (20 μM), the emission at 570 nm (λ_{ex} = 540 nm) is increased 2.4, 12 or 21 fold, correspondingly (Fig. 2A). The sensitivity limit of the system under these conditions is 500 nM Cu^{2+}.

In cells, the reagent BuCh can potentially be exposed to Cu^{2+} in physically isolated intracellular pools, which have different pH's: $e.g.$, 4.5 to 6 in lysosomes, 7.7 to 8.0 in mitochondria and 7.4 in cytoplasm. We investigated the response of BuCh (5 μM) at the representative pH values found in the mentioned intracellular sites (Fig. 2B). We observed that the fluorescence increase (λ_{ex} = 540 nm, λ_{em} = 570 nm) is maximal
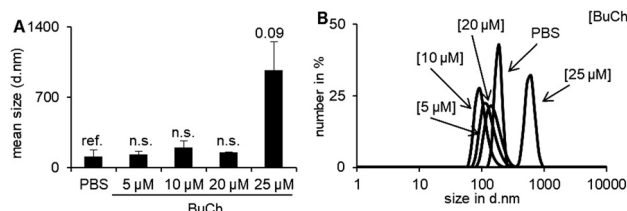
Fig. 1 (A) Mean particle sizes (nm) of aggregated species detected by dynamic light scattering (DLS) in solutions of increasing concentrations of BuCh (5, 10, 20, and 25 μM) in PBS (10 mM, pH 7.4, EtOH 1% v/v). PBS lacking BuCh was used as a reference. Statistical significance was determined using the unpaired Student's t-test, where * – p < 0.05 and n.s. – not significant, $p \geq 0.05$. (B) Representative raw data used to obtain the data shown in the left plot.

Scheme 2 Synthesis of chemodosimeter BuCh: (a) hydrazide hydrate in ethanol at reflux, 17 h; (b): 1-bromobutane, Cs_2CO_3, and CsI in DMF at reflux, 16 h.

Fig. 2 (A) Fluorescence spectra ($\lambda_{ex.}$ = 540 nm) of BuCh (20 μM) in PBS (10 mM, pH 7.4, 1% EtOH, v/v) incubated for 10 min with Cu(OAc)$_2$ (0–9 μM, the concentration was increased in 0.5 μM steps). Signal values are reported in relative units (r.u.), $i.e.$ the raw output of the instrument under fixed gain and integration settings. (B) Fluorescence spectra ($\lambda_{ex.}$ = 540 nm) of mixtures of BuCh (20 μM) and Cu(OAc)$_2$ (5 μM) in different buffers: pH 7.4 (PBS, 10 mM), 8.0 (PBS, 10 mM), 5.5 (NaOAc, 10 mM); incubation time: 10 min. (C) Fluorescence of solution of BuCh (10 μM) in PBS (10 mM, pH 7.4, 1% EtOH, v/v) incubated with different Cu(OAc)$_2$ concentrations (2, 5, 10, 25, and 50 μM) for 12 h at 37 °C. A control labelled on the plot as "EDTA" – N,N,N',N'-ethylenetetraacetic acid (EDTA, 0.1 mM) was added to the mixture of BuCh (10 μM) and Cu(OAc)$_2$ (50 μM). (D) Normalized fluorescence intensity (the expression F_0 describes the fluorescence intensity at time t = 0 min and F describes the fluorescence intensity at the end point t = 180 min, λ_{ex} = 540 nm, λ_{em} = 570 nm) of BuCh (10 μM) in PBS (10 mM, pH 7.4, 1% EtOH, v/v) after the addition of either various metal ions (indicated on the plot) or the carrier ("EtOH") and an incubation time of 3 hours at 37 °C. Statistical significance was determined using the Student's t-test, where * – $p < 0.05$, ** – $p < 0.01$, *** – $p < 0.005$ and not significant (n.s.) – $p \geq 0.05$.

at the typical for cytoplasm pH of 7.4 ($F_{10\ min}/F_0$ = 12), whereas it is strongly decreased at both mitochondrial pH of 8.0 ($F_{10\ min}/F_0$ = 2.8) and lysosomal pH of 5.5 ($F_{10\ min}/F_0$ = 2.6). These data indicate that BuCh is mostly suitable for monitoring Cu^{2+} in cytoplasm.

Next, we studied the effect of long term incubation for detection of Cu^{2+} by using BuCh. We found that the fluorescence of the solution of BuCh (10 μM) in PBS (10 mM, pH 7.4) is increased 2.8 fold after incubation for 12 h. The same increase is observed in the presence of N,N,N',N'-ethylenediaminetetraacetic acid (EDTA, 100 μM). EDTA should bind and block residual Cu^{2+}, which can potentially be present in the PBS medium. These data indicate the limited Cu^{2+} independent hydrolysis of BuCh over 12 h. Due to the spontaneous hydrolysis, the limit of detection of Cu^{2+} is increased to 5 μM at 12 h incubation time (Fig. 2C). The fluorescence increase is practically saturated after addition of 10 μM Cu^{2+} to 10 μM BuCh indicating 1 to 1 stoichiometry of the reaction of the metal ion with the chemodosimeter as expected based on the suggested mechanism of activation (Scheme 1A).

Importantly, we observed that the fluorescence of BuCh is increased only in the presense of Cu^{2+} ions (Student's t test, $p < 10^{-3}$), whereas other biologically relevant metal ions Fe^{2+},

Fe^{3+}, Zn^{2+}, Ni^{2+}, Mg^{2+}, Ca^{2+} and K$^+$ do not affect the fluorescence of this reagent (Fig. 2D). In the case of Cu$^+$, an increase of the fluorescence signal was also apparent. However, it was not statistically significant (p = 0.131). This observation can be explained by the fact that the salt Cu$^+$ triflate used in the latter experiment partially disproportionated to Cu and Cu^{2+} in aqueous solution or directly oxidized by air to Cu^{2+}.

Monitoring Cu^{2+} in living cells using BuCh chemodosimeter

A. T. Pezacki $et\ al.$[27] demonstrated that divalent metal transporter 1 (DMT1, ENSG00000110911) predominantly mediates the cellular uptake of extracellular Cu^{2+} in cell cultures, whereas copper transporter 1 (CTR1, ENSG00000136868) facilitates the import of Cu$^+$. To evaluate the capacity of BuCh to detect intracellular Cu^{2+}, we employed human ovarian carcinoma A2780 cells, which exhibit robust expression of DMT1 (39.1 normalized transcript expression values, nTRM):[38,39] DMT1^{high} cell line. Incubation of A2780 cells with Cu^{2+} salts was therefore anticipated to elevate intracellular Cu^{2+} levels. As a negative control, we utilized human lung squamous cell carcinoma SK-MES-1 cells, characterized by markedly lower DMT1 expression (14.5 nTPM): DMT1^{low} cell line. In addition, human lung fibroblast GM01379 cells were included as a non-malignant control. Although transcriptomic data regarding DMT1 expression in GM01379 cells are unavailable, their non-transformed status suggests a comparatively reducing intracellular environment. Consequently, exposure of GM01379 cells to Cu^{2+} salts was expected to yield only minimal, if any, increases in intracellular Cu^{2+} concentrations.

Accumulation of Cu^{2+} in cells leads to increased oxidative stress, reflected by elevated intracellular levels of reactive oxygen species (ROS). We used this phenomenon as indirect evidence of Cu^{2+} uptake. Specifically, among the tested cell lines (A2780, SK-MES-1, and GM01379), incubation with Cu(OAc)$_2$ induced a rise in intracellular ROS exclusively in A2780 cells (Fig. 3). These findings validate A2780 as the appropriate
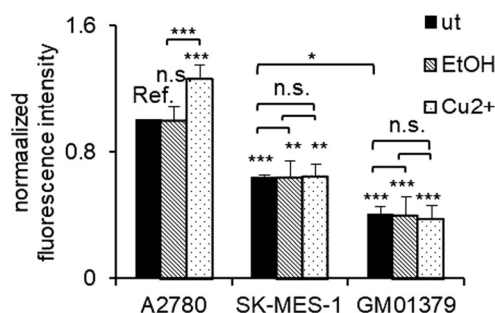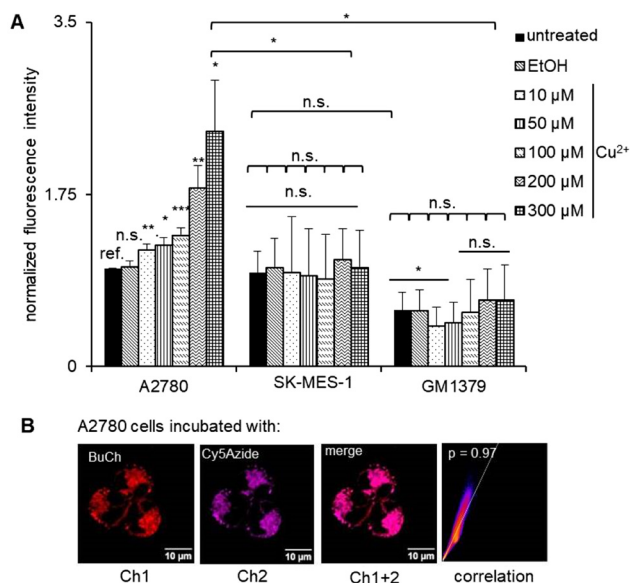

Fig. 3 Change of fluorescence ($\lambda_{ex.}$ = 488 nm and $\lambda_{em.}$ = 585 ± 42 nm) of ROS sensing probe MitoSOX™ (5 μM)-loaded cells (A2780, SK-MES-1, and GM013789) that were either untreated (ut.), pre-treated with the carrier ethanol (EtOH, 1%, v/v), or Cu(OAc)$_2$ (100 μM, 1% EtOH, v/v) for 24 h. Untreated A2780 cells were used as a reference. Their fluorescence was set to 1. Statistical significance was determined using the Student's t-test, where * – $p < 0.05$, ** – $p < 0.01$, *** – $p < 0.005$ and not significant (n.s.) – $p \geq 0.05$.

experimental model, while SK-MES-1 and GM01379 serve as suitable negative control cell lines.

The cells were either left untreated or treated with increasing concentrations of Cu(OAc)$_2$ for 24 h, followed by incubation with BuCh (20 μM) in Hank's Balanced Salt Solution (HBSS) at 37 °C for 1 h. The fluorescence of living, treated, and untreated cells was subsequently quantified by flow cytometry. As expected, BuCh-loaded DMT1^{high} A2780 cells exhibited a significant increase in fluorescence upon incubation with Cu(OAc)$_2$ (Fig. 4A and S10).

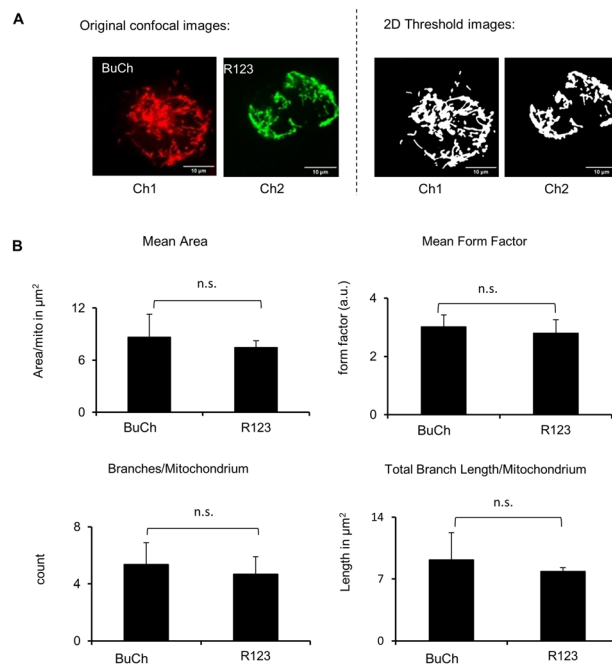The lowest concentration of Cu(OAc)$_2$ that produced a statistically significant increase was 10 μM, resulting in a 1.2-fold elevation in fluorescence. A clear dose-dependent trend was observed, with fluorescence reaching a 2.4-fold increase at 300 μM Cu(OAc)$_2$. In contrast, addition of Cu(OAc)$_2$ did not lead to an increase in fluorescence in BuCh-loaded control DMT1^{low} SK-MES-1 cancer cells (Fig. 3A). This result was anticipated, as these cells express markedly lower levels of the DMT1 transporter, which is essential for extracellular Cu^{2+} uptake.[27] Similarly, Cu(OAc)$_2$ failed to enhance fluorescence in BuCh-loaded healthy GM01379 cells. This outcome was also expected, since these cells maintain a reductive intracellular environment that favours the reduction of Cu^{2+}, thereby preventing its accumulation.

Direct comparison of the previously known chemodosimeter HCh and our optimized one BuCh confirms superiority of the BuCh in the detection of intracellular Cu^{2+} in A2780 cells (Fig. S11).

Confocal fluorescence microscopy of A2780 cells treated with BuCh (Ch1) and co-incubated with the reported mitochondria targeting fluorescent dye Cy5Azide[40] (Ch2) for 30 minutes showed strong co-localization of both signals: Pearson's coefficient −0.97 (Fig. 4B and S12). This suggests that the subcellular location of the fluorescent product after Cu^{2+}-dependent activation of BuCh is the mitochondria of the cells. To evaluate the cytotoxic properties of BuCh and derived from this compound products, we analysed the mitochondrial morphology of the treated A2780 cells and compared it with the established mitochondrial dye Rhodamine 123 (R123). As shown in Fig. 5, there are no significant differences between the morphological properties of the mitochondria (such as mean area, mean shape factor, branches per mitochondrion, and total length of branches per mitochondrion) of cells treated with either BuCh (20 μM, 30 min) or R123 (1 μM, 20 min). This suggests that both reagents exhibit comparable low cytotoxicity at the respective working concentrations. Thus, BuCh is a safe Cu^{2+} responsive chemodosimeter for applications in living cells.

Fig. 4 (A) Change of fluorescence ($\lambda_{ex.}$ = 488 nm and $\lambda_{em.}$ = 585 ± 42 nm) of BuCh (20 μM)-loaded cells (A2780, SK-MES-1, and GM013789 all in RPMI 1640 medium) that were either untreated (ut.), pre-treated with the carrier ethanol (EtOH, 1%, v/v), or Cu(OAc)$_2$ (10, 50 100, 200 and 300 μM, 1% EtOH, v/v) for 24 h. Untreated, BuCh (20 μM)-loaded A2780 cells were used as a reference. Their fluorescence was set to 1. Statistical significance was determined using the Student's t-test, where * − p < 0.05, ** − p < 0.01, *** − p < 0.005 and not significant (n.s.) − p ≥ 0.05. (B) Confocal microscopy images of A2780 cells treated with BuCh (20 μM, $\lambda_{ex.}$ = 561 nm, $\lambda_{em.}$ = 629 ± 62 nm, Ch1) and mitochondria targeting Cy5Azide (10 μM, $\lambda_{ex.}$ = 635 nm, $\lambda_{em.}$ = 690 ± 50 nm, Ch2) for 30 min.

Fig. 5 (A) Exemplary confocal fluorescent microscopy images of A2780 cells treated with either BuCh (20 μM, $\lambda_{ex.}$ = 561 nm, $\lambda_{em.}$ = 629 ± 62 nm, Ch1) or Rhodamine 123 (R123, 1 μM, $\lambda_{ex.}$ = 488 nm, $\lambda_{em.}$ = 525 ± 25 nm, Ch2) for 30 and 20 min respectively, and their corresponding 2D Threshold images which were used for the morphology analysis (B) analysed parameters (mean area, mean form factor, branches per mitochondrium and total branch length per mitochondrium) of the mitochondria morphology analysis of BuCh and R123 treated A2780 cells, using 2D threshold images. Statistical significance was determined using the Student's t-test, where not significant (n.s.) − p ≥ 0.05.

Conclusions

In conclusion, we successfully prepared a new chemodosimeter, BuCh, which is soluble in aqueous solutions at pH 7.4 up to 20 μM and remains non-aggregated under these conditions. Unlike the parent chemodosimeter HCh and its improved analogue PhCh,[37] BuCh exhibits superior cell membrane permeability that enables the detection of intracellular chelatable Cu^{2+} at the chemodosimeter concentration as low as 20 μM, which is not toxic to cells. Owing to its straightforward synthesis from inexpensive starting materials, broad accessibility, and excellent performance, BuCh represents a valuable reagent for laboratories of all scales, including those with limited resources, that rely on the detection of intracellular Cu^{2+}.

Methods and materials

General

Commercially available chemicals of the best quality from Sigma-Aldrich (Germany), Fisher Scientific (Germany) and ChemPur (Germany) were obtained and used without purification. NMR spectra were acquired on a Bruker Avance 300 or a Bruker Avance 400 spectrometer. Atmospheric pressure photoionization (APPI) mass spectra were recorded on a Bruker ESI MicroTOF II focus or a Bruker maXis 4G. Elemental analysis (C, H, and N) was performed in the microanalytical laboratory of the chemical institutes of the Friedrich-Alexander-University of Erlangen-Nürnberg, Erlangen, Germany. UV-visible spectra were measured on a Cary 100 UV-Vis Spectrophotometer (Agilent Technologies) by using either quartz glass cuvettes (Hellma GmbH, Germany) with a sample volume of 1 mL. Fluorescence spectra were acquired on a Varian Cary Eclipse fluorescence spectrophotometer using fluorescence cuvettes (Hellma GmbH, Germany) with a sample volume of 1 mL or on a Thermo Scientific™ Varioskan™ LUX plate reader (US) using 96-well plates with a sample volume of 200 μl per well. The fluorescence of live cells was quantified using a CytoFlex S flow cytometer from Beckman Coulter, Inc. The data were processed using the CyteExpert software package from Beckman Coulter and Microsoft Excel. Confocal images were taken at the Optical Imaging Center Erlangen (OICE) using a Zeiss Spinning Disk Axio Observer Z1 with Plan-Apochromat 63×/1.40 oil objective in spinning disc confocal mode using the Axiocham camera. The purity of the compounds used in the biological assays was determined by elemental analysis (C, H, and N analysis). According to these data, the purity was greater than 95%. Statistical analysis of the data was conducted using unpaired Student's t-test when not stated otherwise. Two data sets were considered significantly different from each other for $p < 0.05$.

Synthesis

Synthesis of rhodamine B hydrazide (HCh). This adapted procedure has been described elsewhere.[41]

In a flask, hydrazine hydrate (95.4 μl, 1.91 mmol, 3.58 equiv.) was dissolved in ethanol (2 mL), afterwards Rhodamine B (0.255 g, 0.532 mmol, 1 equiv.) was added. The reaction mixture was stirred for 17 h at reflux temperature. The solvent was evaporated, re-dissolved in ethyl acetate (2 mL) and washed with aq. sodium hydrogen carbonate (3 × 3 mL, pH 9), the combined organic phases were dried over magnesium sulfate and the remaining solvent evaporated. The crude product was purified via Silica gel column chromatography (cyclohexane/ethyl acetate 2/1, v/v) and rhodamine B hydrazide could be obtained as a light pink solid (0.138 g, 57%). ^{1}H NMR spectroscopy (300 MHz, acetone) δ 7.83–7.76 (m, 1H), 7.53–7.44 (m, 2H), 7.06–7.00 (m, 1H), 6.45–6.34 (m, 6H), 4.01 (d, J = 6.4 Hz, 2H), 3.40 (q, J = 7.0 Hz, 8H), 1.16 (t, J = 7.0 Hz, 12H). Elemental analysis, calcd for $C_{28}H_{32}N_4O_2$: C [%] = 73.66, N [%] = 12.27, H [%] = 7.06, found C [%] = 73.80, N [%] = 12.12, H [%] = 7.19.

Synthesis of 2-(butylamino)-3′,6′-bis(diethylamino)spiro [isoindo-line-1,9′-xanthen]-3-one (BuCh). Rhodamine B hydrazide (0.138 g, 0.303 mmol, 1 equiv.), 1-bromobutane (65.3 μl, 0.606 mmol, 2 equiv.), Cs_2CO_3 (0.296 g, 0.908 mmol, 3 equiv.) and CsI (0.118 g, 0.454 mmol, 1.5 equiv.) were dissolved in N,N-dimethylformamide (3 mL) and stirred for 16 h at reflux temperature. Afterwards the solvent was evaporated, re-dissolved in ethyl acetate (3 mL) and washed with deionized water (3 × 3 mL). The organic phase was dried over magnesium sulfate and the remaining solvent evaporated in vacuo (0.1 bar). The crude product was purified via aluminium oxide (ALOX) gel column chromatography (cyclohexane/ethyl acetate 2/1, v/v). BuCh was obtained as a light pink solid (0.067 g, 49%). ^{1}H NMR spectroscopy (300 MHz, acetone) δ 7.85–7.78 (m, 1H), 7.61–7.47 (m, 2H), 7.12–7.05 (m, 1H), 6.43–6.33 (m, 6H), 4.28 (d, J = 6.6 Hz, 1H), 3.40 (q, J = 7.0 Hz, 8H), 2.58 (dd, J = 6.7, 5.4 Hz, 2H), 1.19–1.13 (m, 12H), 1.09 (dd, J = 7.9, 4.4 Hz, 4H), 0.74–0.61 (m, 3H). ^{13}C NMR (101 MHz, acetone) δ 165.64, 153.96, 151.61, 148.63, 132.35, 131.27, 128.45, 128.12, 123.95, 122.11, 107.71, 106.66, 97.71, 65.00, 50.33, 44.01, 30.22, 19.71, 13.23, 11.98. HR—APPI-MS (positive mode): m/z calcd 513.3221 for $C_{32}H_{40}N_4O_2$ $[M + H]^+$, found 513.3226. Elemental analysis, calcd for $C_{32}H_{40}N_4O_2 \cdot 2H_2O$: C [%] = 70.04, N [%] = 10.21, H [%] = 8.08, found C [%] = 70.68, N [%] = 9.92, H [%] = 7.62.

Solubility in aqueous solutions

The analyzed dilutions were either prepared in phosphate-buffered saline (PBS, 990 μl phosphate (10 mM), NaCl (150 mM), pH = 7.4) or RPMI 1640 medium (990 μl) with 5% fetal bovine serum (FBS), 1% L-glutamine (Gln), 1% penicillin/streptomycin (Pen/Strep). Stock solutions with different concentrations of BuCh were dissolved in EtOH (10 μL) and added to the aqueous solutions in the 1 mL quartz cuvette (1% EtOH v/v). The absorbance at 789 nm and 250 nm of the solutions/suspensions (A789 nm, A250 nm) was measured and plotted as a function of the concentration of the solutions/suspensions. The solubility limit was analyzed as follows: an absorbance at A789 that is less than or equal to 2 times of the absor-

bance A789 of the blank solution. The absorbance at A250 follows Lambert Beer's law when plotted against the concentration. Turbidity of the solution was also considered a criterion for insolubility.

log P (octanol–water partition coefficient)

Reversed-phase (RP)-TLC plates from Macherey-Nagel (Germany, Alugram Aluminiumfolien RP-18 W/UV254, stationary phase thickness: 0.15 mm) were used for determination of $\log P$ values. Mixtures of aqueous 3-(N-morpholino)propanesulfonic acid buffer (MOPS, 100 mM, pH 7.4) and acetonitrile (1/2 and 2/3 and 2/3.5, v/v) were used as eluents. Phenlyboricacid ($\log P = 1.59$), benzophenone ($\log P = 3.18$), anthracene ($\log P = 4.45$), pyrene ($\log P = 4.88$) and perylene ($\log P = 6.25$) were used as reference compounds with known $\log P$ values. Freshly prepared solutions of the sample and references (in acetone) were spotted on the RP-TLC plates. The spots of the compounds were monitored by using UV-imaging. Each spot was marked and its position relative to the start line (Lc) was measured. R_f – values were calculated as ratio of Lc to L (end line). Calibration plots of R_f versus $\log P$ values for the known compounds were used for determination of the $\log P$ value of BuCh. All measurements were done in triplicates.

Dynamic light scattering (DLS)

DLS was measured with a Zetasizer Nano ZS (Red badge, ZEN3600, Malvern Panalytical Ltd) by using disposable cuvettes (polystyrene) with a sample volume of 2.5 mL. DLS of solutions of the compound BuCh (1 μM, 5 μM, 10 μM, 20 μM and 25 μM) in PBS buffer (10 mM, pH 7.4, 1% EtOH, v/v) and RPMI 1640 (5% FBS, 1% Gln and 1% Pen/Strep, 1% EtOH, v/v) were determined under the following settings: 25 °C, solvent: PBS (RI: 1.330; viscosity (cP): 0.9200) and water (for RPMI medium, RI: 1.330; viscosity (cP): 0.9200) (for analysis: (RI: 1.45; material absorption: 0.220); backward scatter; 3 measurements per sample).

Fluorescence titration measurement with Cu^{2+}

Fluorescence measurements were performed in fluorescent cuvettes with a capacity of 1 mL. BuCh (final concentration 20 μM) was dissolved in either PBS (10 mM, pH 7.4, 1% EtOH, v/v), PBS (10 mM, pH 8.0, 1% EtOH) or sodium acetate buffer (100 mM, pH 5.5, 1% EtOH, v/v) and measured at $\lambda_{ex.} = 540$ nm and an emission range of 550 to 750 nm. Subsequently, 1 μl Cu(OAc)$_2$ (0.5 mM in EtOH, final concentration per addition 0.5 μM, 0.1% EtOH, v/v) was added successively up to a final concentration of 9 μM, incubated each addition for 10 min.

Fluorescence long term measurement with Cu^{2+}

Fluorescence measurements over a longer period of time were performed in 96-well plates with a sample volume of 200 μl per well on a Thermo Scientific™ Varioscan™ LUX plate reader (US) at a set $\lambda_{ex.} = 540$ nm and $\lambda_{em.} = 570$ nm over a period of 12 hours at 37 °C, with measurements taken every 25 minutes. BuCh (20 μM) was measured in PBS (10 mM, pH

7.4, 1% EtOH, v/v) without Cu(OAc)$_2$ addition or with different concentrations of Cu(OAc)$_2$ (2 μM, 5 μM, 10 μM, 20 μM, 50 μM) or with Cu(OAc)$_2$ (50 μM) and EDTA (0.1 mM) as a negative control.

Fluorescence measurement with different metal Ions

Fluorescence measurements were performed in 96-well plates with a sample volume of 200 μl per well on a Thermo Scientific™ Varioscan™ LUX plate reader (US) at a set $\lambda_{ex.} = 540$ nm and $\lambda_{em.} = 570$ nm over a period of 3 hours at 37 °C, with measurements taken every 13 minutes. BuCh (10 μM) in PBS (10 mM, pH 7.4, 1% EtOH, v/v) was either mixed with different metal salts (0.5 mM FeCl$_3$, 0.5 mM ZnI$_2$, 0.5 mM NiCl$_2$, 0.2 mM Cu(OAc)$_2$, 0.5 mM FeCl$_2$, 1 mM MgCl$_2$, 0.2 mM CuOTf, 150 mM KCl and 1 mM CaCl$_2$) or without salt addition (ref.) and the fluorescence was measured.

Cells and cell culture

Cells were cultured according to recommendations of Deutsche Sammlung von Mikroorganismen und Zellkulturen GmbH (DSMZ). Human ovarian carcinoma A2780 (Sigma Aldrich) cell line was grown in Roswell Park Memorial Institute (RPMI) 1640 medium (Biochrom GmbH, Germany) medium with 10% fetal bovine serum (FBS, Biochrom GmbH, Germany), 1% L-glutamine, and 1% penicillin/streptomycin (Pen/Strep). SK-MES-1 cell line was purchased from CLS Cell Lines Service GmbH, Eppelheim (Germany) and GM01379 Human Lung GM01379 fibroblasts were a kind gift of Prof. Dr Ivana Ivanovic-Burmazovic (Bioinorganic Chemistry and Coordination Chemistry Ludwig–Maximilians–University Munich, Germany). They were cultivated in Dulbecco's modified Eagle's medium (DMEM, Biochrom GmbH, Germany) medium, all supplemented with 10% FBS, 1% L-glutamine, and 1% pen/strep. Adherent A2780, SK-MES-1 and GM01379 cells were cultivated to 70–80% confluence. For passaging and experimental setup, the adherent cells were detached from culture flasks (trypsination) by using a mixture of trypsin (0.025%, w/v) and EDTA (0.02%, w/v) in PBS buffer.

Cu^{2+} detection in different human cell lines

A2780 were seeded at a concentration of 250 cells per μL in RPMI 1640 medium with 5% FBS, 1% Gln and 1% PEN/STREP, SK-MES-1 and GM01379 were seeded at a concentration of 200 cells per μL and 125 cells per μL, respectively, in either DMEM medium with 5% FBS, 1% Gln and 1% PEN/STREP or in RPMI 1640 medium as well, in a 96-well plate (100 μL per well). The cells were allowed to adhere overnight at 37 °C and 5% CO$_2$. Subsequently, the cells were treated with Cu(OAc)$_2$ to final concentrations of 10 μM, 50 μM, 100 μM and 300 μM (1% EtOH, v/v). After 24 h incubation, the cells were washed twice with DPBS (100 μL per well) and BuCh (20 μM in HBSS, 1% EtOH v/v) or HCh (20 μM in HBSS, 1% EtOH, v/v) was added and incubated for 1 h at 37 °C. Subsequently, the cells were washed again, trypsinated using trypsin/EDTA (0.25% trypsin, v/v, 100 μl) and re-suspended in fresh medium (100 μL). Finally, the fluorescence of the living cells ($\lambda_{ex.} =$

488 nm, $\lambda_{em.}$ = 585 ± 42 nm) in the suspensions was determined by using flow cytometry which was performed on the CytoFLEX S Flow Cytometer from Beckmann Coulter (U.S.) and analyzed with the CytExpert version 2.4 from Beckmann Coulter (U.S.).

Mitochondrial ROS (mROS) detection in different human cell lines

A2780 cells were seeded at a concentration of 250 cells per µl in RPMI 1640 (5% FBS, 1% Gln and 1% Pen/Strep), SK-MES-1 and GM01379 cells at a concentration of 200 cells per µl and 125 cells per µl in DMEM (5% FBS, 1% Gln and 1% Pen/Strep) in 96-well plates (100 µl per well) and allowed to attach overnight at 37 °C and 5% CO_2. To determine their mitochondrial ROS (mROS) the cells were treated with different $Cu(OAc)_2$ concentrations (10 µM, 100 µM, and 300 µM, 1% EtOH, v/v) and ethanol only (1% v/v) and incubated for 24 hours. The medium was then removed, the cells were washed twice with DPBS (100 µl per well), and the mROS sensor was added to the cells in HBSS (mROS: MitoSOX, 5 µM, 0.1% DMSO, v/v) and incubated for 20 min. The cells were then washed again, trypsinized, resuspended in fresh medium (100 µl per well), and the fluorescence of living cells ($\lambda_{ex.}$ = 488 nm, $\lambda_{em.}$ = 585 ± 42 nm) was analyzed immediately afterwards using a CytoFlex S flow cytometer.

Confocal microscopy experiments

A2780 cells were seeded at a cell concentration of 80 cells per µl in imaging dishes (µ-Dish 35 mm, high, ibidi GmbH, Germany; 500 µl per dish) in RPMI 1640 medium (5% FBS, 1% Gln, and 1% Pen/Strep) and allowed to attach overnight at 37 °C and 5% CO_2.

Determination of subcellular distribution

The cells were then washed with DPBS (2 mL per dish) and incubated with BuCh (20 µM) and Cy5Azide (10 µM) together in HBSS, 1% EtOH, v/v for 30 min. The cells were washed again with DPBS and covered with fresh medium (2 mL per dish). Confocal fluorescence images of the cells were immediately recorded (BuCh: $\lambda_{ex.}$ = 561 nm, $\lambda_{em.}$ = 629 ± 62 nm red channel; Cy5Azide: ($\lambda_{ex.}$ = 635 nm, $\lambda_{em.}$ = 690 ± 50 nm, magenta channel)) with a Zeiss Spinning Disk Axio Observer Z1 with Plan-Apochromat 63×/1.40 oil objective in spinning disc confocal mode using the Axiocham camera.

Mitochondrial morphology

The cells were then washed with DPBS (2 mL per dish) and incubated with either BuCh (20 µM in HBSS, 1% EtOH, v/v) for 30 min or Rhodamine 123 (R123, 1 µM in HBSS, 0.1% DMSO, v/v) for 20 min. The cells were washed again with DPBS and covered with fresh medium (2 mL per dish). Confocal fluorescence images of the cells were immediately recorded (BuCh: $\lambda_{ex.}$ = 561 nm, $\lambda_{em.}$ = 629 ± 62 nm red channel; R123: $\lambda_{ex.}$ = 488 nm, $\lambda_{em.}$ = 525 ± 25 nm, green channel) with a Zeiss Spinning Disk Axio Observer Z1 with Plan-Apochromat 63×/1.40 oil objective in spinning disc confocal mode using the

Axiocham camera. The morphology of the mitochondria was analyzed using the "Mitochondria Analyzer" plugin of the image editing software ImageJ/Fiji,[42] whereby 2D Threshold images of the respective mitochondria were created and these were examined and compared with regard to various attributes.

Author contributions

Conceptualization: AM; methodology: AM, MK; conducting experiments: MK, DA, EKM; data curation and analysis: MK, DA, AM; writing – original draft: MK, AM. writing – review and editing: AM, MK.

Conflicts of interest

There are no conflicts to declare.

Data availability

The data supporting this article have been included as part of the supplementary information (SI). Supplementary information is available. See DOI: https://doi.org/10.1039/d5dt02331a

Acknowledgements

References

1 P. C. Wong, D. Waggoner, J. R. Subramaniam, L. Tessarollo, T. B. Bartnikas, V. C. Culotta, D. L. Price, J. Rothstein and J. D. Gitlin, *Proc. Natl. Acad. Sci. U. S. A.*, 2000, **97**, 2886–2891.

2 N. E. Hellman and J. D. Gitlin, *Annu. Rev. Nutr.*, 2002, **22**, 439–458.

3 E. I. Solomon, U. M. Sundaram and T. E. Machonkin, *Chem. Rev.*, 1996, **96**, 2563–2606.

4 M. Bonham, J. M. O'Connor, B. M. Hannigan and J. J. Strain, *Br. J. Nutr.*, 2002, **87**, 393–403.

5 J. Y. Uriu-Adams and C. L. Keen, *Mol. Aspects Med.*, 2005, **26**, 268–298.

6 D. Tang, G. Kroemer and R. Kang, *Nat. Rev. Clin. Oncol.*, 2024, **21**, 370–388.

7 C.-J. Lin, H.-C. Huang and Z.-F. Jiang, *Brain Res. Bull.*, 2010, **82**, 235–242.

8 G. R. Thomas, J. R. Forbes, E. A. Roberts, J. M. Walshe and D. W. Cox, *Nat. Genet.*, 1995, **9**, 210–217.

9 D. J. Waggoner, T. B. Bartnikas and J. D. Gitlin, *Neurobiol. Dis.*, 1999, **6**, 221–230.

10 P. C. Bull, G. R. Thomas, J. M. Rommens, J. R. Forbes and D. W. Cox, *Nat. Genet.*, 1993, **5**, 327–337.

11 A. K. Baltaci, T. K. Dundar, F. Aksoy and R. Mogulkoc, *Biol. Trace Elem. Res.*, 2017, **175**, 57–64.

12 S. Basu, M. K. Singh, T. B. Singh, S. K. Bhartiya, S. P. Singh and V. K. Shukla, *World J. Surg.*, 2013, **37**, 2641–2646.

13 M. Stepien, M. Jenab, H. Freisling, N.-P. Becker, M. Czuban, A. Tjønneland, A. Olsen, K. Overvad, M.-C. Boutron-Ruault, F. R. Mancini, I. Savoye, V. Katzke, T. Kühn, H. Boeing, K. Iqbal, A. Trichopoulou, C. Bamia, P. Orfanos, D. Palli, S. Sieri, R. Tumino, A. Naccarati, S. Panico, H. B. Bueno-de-Mesquita, P. H. Peeters, E. Weiderpass, S. Merino, P. Jakszyn, M.-J. Sanchez, M. Dorronsoro, J. M. Huerta, A. Barricarte, S. Boden, B. van Guelpen, N. Wareham, K.-T. Khaw, K. E. Bradbury, A. J. Cross, L. Schomburg and D. J. Hughes, *Carcinogenesis*, 2017, **38**, 699–707.

14 L. Jouybari, F. Kiani, F. Islami, A. Sanagoo, F. Sayehmiri, B. Hosnedlova, M. D. Doşa, R. Kizek, S. Chirumbolo and G. Bjørklund, *Curr. Med. Chem.*, 2020, **27**, 6373–6383.

15 M. Taki, S. Iyoshi, A. Ojida, I. Hamachi and Y. Yamamoto, *J. Am. Chem. Soc.*, 2010, **132**, 5938–5939.

16 C. Y.-S. Chung, J. M. Posimo, S. Lee, T. Tsang, J. M. Davis, D. C. Brady and C. J. Chang, *Proc. Natl. Acad. Sci. U. S. A.*, 2019, **116**, 18285–18294.

17 A. T. Pezacki, J. Gao and C. J. Chang, *Curr. Opin. Chem. Biol.*, 2024, **83**, 102541.

18 L. Zeng, E. W. Miller, A. Pralle, E. Y. Isacoff and C. J. Chang, *J. Am. Chem. Soc.*, 2006, **128**, 10–11.

19 J. Huang, M. Liu, X. Ma, Q. Dong, B. Ye, W. Wang and W. Zeng, *RSC Adv.*, 2014, **4**, 22964–22970.

20 H. Chen, P. Yang, Y. Li, L. Zhang, F. Ding, X. He and J. Shen, *Spectrochim. Acta, Part A*, 2020, **224**, 117384.

21 M. Cao, L. Jiang, F. Hu, Y. Zhang, W. C. Yang, S. H. Liu and J. Yin, *RSC Adv.*, 2015, **5**, 23666–23670.

22 Y. Hu, A. Chen, Z. Kong and D. Sun, *Molecules*, 2019, **24**, 4283.

23 L. Liu, T. Zhou, Y. Li and T. Li, *J. Fluoresc.*, 2025, **35**, 5807–5816.

24 Y.-Z. Chen and H.-L. Jiang, *Chem. Mater.*, 2016, **28**, 6698–6704.

25 T. Rasheed, F. Nabeel, M. Adeel, M. Bilal and H. M. N. Iqbal, *Biocatal. Agric. Biotechnol.*, 2019, **17**, 696–701.

26 M. Tian, H. He, B.-B. Wang, X. Wang, Y. Liu and F.-L. Jiang, *Dyes Pigm.*, 2019, **165**, 383–390.

27 A. T. Pezacki, C. D. Matier, X. Gu, E. Kummelstedt, S. E. Bond, L. Torrente, K. L. Jordan-Sciutto, G. M. DeNicola, T. A. Su, D. C. Brady and C. J. Chang, *Proc. Natl. Acad. Sci. U. S. A.*, 2022, **119**, 43.

28 C.-Y. Chou, S.-R. Liu and S.-P. Wu, *Analyst*, 2013, **138**, 3264.

29 Y. Zhang, Z. Liu, K. Yang, Y. Zhang, Y. Xu, H. Li, C. Wang, A. Lu and S. Sun, *Sci. Rep.*, 2015, **5**, 8172.

30 M. Liu, H. Zhu, K. Wang, X. Zhang, X. Li, M. Yu, B. Zhu, W. Sheng and C. Liu, *ACS Food Sci. Technol.*, 2023, **3**, 134–140.

31 S. Anbu, A. Paul, K. Surendranath, A. Sidali and A. J. L. Pombeiro, *J. Inorg. Biochem.*, 2021, **220**, 111466.

32 Y. Ping, M. Liu, Y. Yu, F. Shang, Q. Chen, Z. Zhang, H. Xu, C. Deng and Y. Li, *J. Fluoresc.*, 2025, 1–10.

33 E. Karakuş, *J. Mol. Struct.*, 2021, **1224**, 129037.

34 L. Zhao, K. Chen, K. Xie, J. Hu, M. Deng, Y. Zou, S. Gao, Y. Fu and F. Ye, *Dyes Pigm.*, 2023, **210**, 110943.

35 V. Dujols, F. Ford and A. W. Czarnik, *J. Am. Chem. Soc.*, 1997, **119**, 7386–7387.

36 C.-M. Wu, Y.-H. Chen, K. Dayananda, T.-W. Shiue, C.-H. Hung, W.-F. Liaw, P.-Y. Chen and Y.-M. Wang, *Anal. Chim. Acta*, 2011, **708**, 141–148.

37 S. K. Kempahanumakkagaari, R. Thippeswamy and P. Malingappa, *J. Lumin.*, 2014, **146**, 11–17.

38 H. Jin, C. Zhang, M. Zwahlen, K. von Feilitzen, M. Karlsson, M. Shi, M. Yuan, X. Song, X. Li, H. Yang, H. Turkez, L. Fagerberg, M. Uhlén and A. Mardinoglu, *Nat. Commun.*, 2023, **14**, 5417.

39 M. Uhlén, L. Fagerberg, B. M. Hallström, C. Lindskog, P. Oksvold, A. Mardinoglu, A. Sivertsson, C. Kampf, E. Sjöstedt, A. Asplund, M. Olsson, K. Edlund, E. Lundberg, S. Navani, C. A. K. Szigyarto, J. Odeberg, D. Djureinovic, O. Takanen, S. Hober, T. Alm, P. H. Edqvist, H. Berling, H. Tegel, J. Mulder, J. Rockberg, P. Nilsson, J. M. Schwenk, M. Hamsten, K. Von Feilitzen, M. Forsberg, L. Persson, F. Johansson, M. Zwahlen, G. Von Heijne, J. Nielsen and F. Pontén, *Science*, 2015, **347**, 6220.

40 S. Chernii, R. Selin, G. Bila, R. Bilyy, M. Körber and A. Mokhir, *Chem. – Eur. J.*, 2024, **30**, 48.

41 F. Abebe, P. Perkins, R. Shaw and S. Tadesse, *J. Mol. Struct.*, 2020, **1205**, 127594.

42 A. Chaudhry, R. Shi and D. S. Luciani, *Am. J. Physiol.: Endocrinol. Metab.*, 2020, **318**, E87–E101.